Promoted electron transport and sustained phonon transport by DNA down to 10 K

CrossMark

Zaoli Xu [a], Xinwei Wang [a, b, *], Huaqing Xie [c]

[a] Department of Mechanical Engineering, Iowa State University, Ames, IA 50011, USA
[b] School of Power and Mechanical Engineering, Wuhan University, Wuhan, Hubei 430072, PR China
[c] School of Urban Development and Environmental Engineering, Shanghai Second Polytechnic University, Shanghai 201209, PR China

ARTICLE INFO

ABSTRACT

This work reports on a pioneering study of the electron transport in nanometer-thick Ir film supported by a DNA fiber, and the phonon transport sustained by the DNA itself. By evaluating the electrical resistivity (ρ_e)~temperature relation based on the Block-Grüneisen theory, we find the Ir film has weak phonon softening indicated by 7–15% Debye temperature reduction. The Ir film's intrinsic ρ_e is promoted by DNA electron thermal hopping and quantum tunneling, and is identical to that of bulk Ir. Although the nanocrystalline structure in ultrathin metallic films intends to give a higher Lorenz number since it reduces the electrical conductivity more than thermal conductivity, the DNA-promoted electron transport in the Ir film preserves a Lorenz number close to that of bulk crystalline Ir. By defining a new physical parameter entitled "thermal reffusivity", the residual phonon thermal resistivity of DNA is identified and evaluated for the first time. The thermal reffusivity concept can be widely used to predict the phonon thermal transport potential of defect-free materials. We predict that the thermal diffusivity of defect-free DNA fiber could be 36–61% higher than the samples studied herein. The structure domain size for phonon diffusion/scattering is determined as 0.8 nm in DNA.

© 2014 Elsevier Ltd. All rights reserved.

1. Introduction

In the last two decades, DNA has served as a promising molecular material with its sequence-specific molecular recognition and self-assembly capabilities to construct nanostructures [1–3]. For its possible application to fabricate nanometer scale electronic devices, the electrical conduction of DNA has been extensively studied. The charge transport through DNA molecules over a few nanometers has been explained by several mechanisms, including coherent quantum tunneling and diffusive thermal hopping [4,5]. These two competing mechanisms are consistent with the Mott variable range hopping electron transport mechanism [6,7], which is revealed in polymer nanostructures, including nanocomposites, nanoparticles, and nanofibers [8–12]. In contrast, studies show that the long-range electron transfer (>50 nm) along DNA is versatile. Some reports that DNA is an insulator [13], while others reveal that DNA is metallically conductive [14] or even superconductive [15]. More results suggest that DNA is a semiconductor [16,17].

Therefore, the electron transfer along DNA molecule is believed to depend on its particular length, base sequence and ambient condition.

Although heat conduction in DNA is also important for designing nanoscale electronic devices, it has not been studied extensively as much as electron conduction. Meanwhile, from the biological perspective, the understanding of thermal conduction is vital to decode DNA denaturation via thermal fluctuations [18]. Only a few report the studies of thermal conduction in DNA recently. By using Peyrard-Bishop-Dauxois (PBD) [18] and 3-D coarse-grained models [19], theoretical results suggest that DNA is indeed a poor heat conduction candidate with a low thermal conductivity. In contrast, measurement on a DNA-gold composite shows a thermal conductivity with 150 W/m·K [20], which is not surprise since the gold coating will have a large thermal effect on the overall thermal transport in metallized DNA. Recently, we report the study of the energy transport in crystalline DNA-composited micro-fibers and films [21]. The thermal conductivity of the DNA-composited fiber is 0.33 W/m·K, and the alignment of DNA molecule results in an enhancement of thermal conductivity (0.63 W/m·K). The thermal conductivity of the DNA-composited film is measured to be around 3 W/m·K, much larger than that of the fiber. The increase is mainly due to the sample structure

difference and the contribution of sodium chloride (NaCl). The same enhancement phenomenon in thermal transport due to DNA structure alignment is also found in the film. The microscale DNA fiber and film do not show extraordinary thermal transport capability, and the DNA molecule structure configuration does have a strong impact on the thermal transport.

In this work, we report an extensive study of the energy transport along the DNA fiber down to very low temperatures. We begin with the description and design of the cryogenic system and thermal characterization technology for the measurement. Variations of thermal conductivity, thermal diffusivity and volumetric heat capacity of the DNA fiber with temperature are reported, respectively. The inverse of thermal diffusivity is introduced as "thermal reffusivity" to evaluate the phonon thermal resistivity, and quantitatively determine the contribution of defect to phonon scattering. Meanwhile, the electrical and thermal conductions of iridium (Ir) nanoscale film are also studied in detail, and DNA-promoted electron transport is observed.

2. Experimental details

2.1. Materials and cryogenic system

The preparation of DNA fiber is detailed in our previous work [21]. Briefly, salmon testes DNA is dissolved and stored in Tris—EDTA (TE) buffer (10 mM Tris—HCl and 1.0 mM EDTA) with NaCl. The concentration is 1 wt% DNA with 1 wt% NaCl. DNA fiber is drawn out of a solution droplet by using a tungsten tip on an electrode, and then attached to the second droplet on another electrode. The drawn fiber is suspended across the electrode gap for thermal transport study, as shown in Fig. 1(a).

Thermal characterization of the DNA fiber is carried out in a cryogenic system [CCS-450, JANIS, Fig. 1(c)]. The system can be used to perform experiments under temperatures as low as 10 K. A closed loop of helium gas is compressed and expanded between the compressor and the cold head. During the expansion phase of each cycle, heat is removed from the cold finger, on which the electrode base with DNA fiber is installed. The cold finger is covered by a radiation shield to block room temperature radiation before it reaches the sample, allowing the lowest possible sample temperature to be achieved. A heater and thermometer are installed on the cold finger and are used to precisely control the sample temperature by a temperature controller. The system is connected to a cold-trapped mechanical vacuum pump to reach a vacuum level as low as 0.3 mTorr, which is needed to eliminate the heat convection effect in the measurement. For the sake of the measurement, the electrode base is electrically insulated from the sample mount by applying a thin cryogenic vacuum grease (Apiezon N Grease) film between them. The grease film also provides a good thermal contact, making the sample temperature very close to that of the cold finger. The electrodes are connected to the electrical feedthroughs by using small gauge wires (32 AWG) for applying current to the sample and for voltage measurement across the sample.
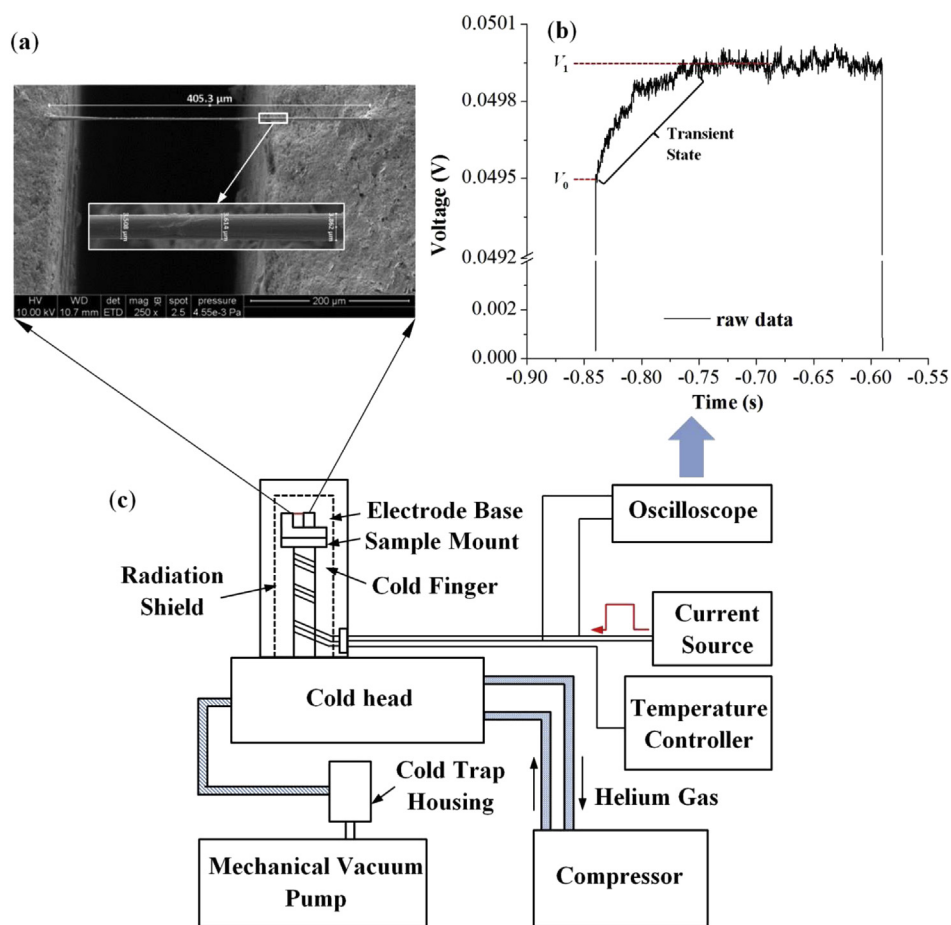
Fig. 1. (a) SEM image of DNA fiber 1. (b) A typical *V-t* profile from the oscilloscope during TET measurement. (c) Schematic of the experimental principle of the transient electro-thermal (TET) technique in the cryogenic system. The electrode base is installed onto the sample mount in the cold finger. The temperature is precisely maintained by a temperature controller. The electrodes are connected to the electrical feedthroughs for applying current to the sample and for voltage measurement across the sample.

2.2. TET characterization of thermal transport in DNA fiber

The thermal properties of DNA fiber are measured by using the transient electro-thermal (TET) technique [22], along with a calibration process by the measurement of temperature-dependent resistance in the cryogenic system. The TET technique has been thoroughly evaluated by measuring the well-known reference materials, and is widely used to measure new materials in our lab [21–24]. The non-conductive DNA fiber is first coated with a 15 nm Ir film (Q150T, Quorum Technologies) to make it electrically conductive. Afterwards, a periodic step DC current is fed through the sample to introduce joule heating. The temperature rise evolution due to the heating can be monitored through the voltage increase recorded by a digital oscilloscope [Fig. 1(b)]. During the heating process, the voltage will increase from the initial value V_0 to the steady state V_1. The transient phase can be used to determine the thermal diffusivity of the sample. The thermal conductivity of the sample can be determined by the steady voltage rise and its temperature coefficient of resistance (TCR) determined by the calibration process between temperature and electrical resistance. More details are provided in Refs. [21,22]. Here we develop the TET technique suitable for the measurement in the cryogenic system.

The heat transfer governing equation for the TET technique is:

$$\rho c_p \frac{\partial T}{\partial t} = k \frac{\partial^2 T}{\partial x^2} + q_0 - 4\varepsilon_r \sigma (T^4 - T_0^4) \Big/ D, \tag{1}$$

where ρc_p and k are the volumetric heat capacity and thermal conductivity of the sample, respectively. q_0 is the electrical heating power per unit volume. $\sigma = 5.67 \times 10^{-8}$ W/m^2 K^4 is the Stefan–Boltzmann constant, and ε_r is the surface emissivity of the Ir-coated sample. For the DNA fiber, only top half of the sample is coated with Ir. The emissivity of the coated half is around 0.04, and the uncoated half is ~0.9 for biomaterials. Thus the overall emissivity is estimated as the average 0.47. D is the sample's average diameter.

To solve the governing equation, the radiation term in Eq. (1) needs to be simplified first. The radiation term is negligible at low temperatures (<150 K), since the radiation power is depressed to only a percentage of the electrical heating power q_0. For the temperatures above, the radiation term can be expressed as $16\varepsilon_r \sigma T_0^3 \theta / D$ by introducing $\theta = T - T_0$ for $\theta \ll T_0$.

First, we seek the steady state solution for the above governing equation. The average steady temperature over the sample length can be written as,

$$T(t \to \infty) = T_0 + \frac{q_0 l^2}{12 k_{real+rad+Ir}}, \tag{2}$$

where l is the sample length, and $k_{real+rad+Ir}$ is effective thermal conductivity. $k_{real+rad+Ir}$ can be obtained by solving Eq. (2) if the steady temperature rise is found. $k_{real+rad+Ir}$ consists of three parts,

$$k_{real+rad+Ir} = k_{real} + \frac{L_{Ir} T l}{RA} + \frac{16\varepsilon_r \sigma T_0^3 l^2}{\pi^2 D}. \tag{3}$$

The first term on the right hand side of Eq. (3) is the thermal conductivity of the DNA fiber. The second term is referred as the "Ir coating effect". L_{Ir} is the Lorenz number of Ir, R is the electrical resistance for the Ir-coated fiber, and A is the cross-sectional area of the fiber. The last term is the "radiation effect".

The transient solution to the governing equation can be expressed in the normalized temperature increase $T^*(t)$, defined as $T^*(t) = [T(t) - T_0]/[T(t \to \infty) - T_0]$,

$$T^* = \frac{96}{\pi^4} \sum_{m=1}^{\infty} \frac{1 - \exp\left[-(2m-1)^2 \pi^2 \alpha_{real+rad+Ir} t \big/ l^2\right]}{(2m-1)^4}, \tag{4}$$

where $\alpha_{real+rad+Ir} = \alpha_{real} + L_{Lorenz} Tl/RA\rho c_p + 16\varepsilon_r \sigma T_0^3 l^2/\rho c_p D\pi^2$. Note that T^* shares the same expression as the normalized voltage increase V^*, which is defined as $[V(t) - V_0]/[V(t \to \infty) - V_0]$. The experimental normalized voltage evolution can be fitted to the theoretical solution $T^*(t)$ with only a single parameter: the effective thermal diffusivity $\alpha_{real+rad+Ir}$. Similar to the steady state solution, α_{real} is the thermal diffusivity of the DNA fiber, and the second and last terms on the right hand side of the expression of $\alpha_{real+rad+Ir}$ are the "Ir coating effect" and "radiation effect". To the end, the volumetric heat capacity of DNA fiber is given by $\rho c_p = k_{real+rad+Ir}/\alpha_{real+rad+Ir}$.

3. Results and discussion

Two DNA fibers are measured down to 10 K in the same manner. The length and average diameter of DNA fiber 1 are 0.405 mm and 3.47 μm, as shown in Fig. 1(a). The length and average diameter of DNA fiber 2 are 0.703 mm and 13.9 μm, respectively. Both fibers are coated with a 15 nm thick Ir film before the test. First, we will present the electron transport in the Ir film on the DNA fiber, and then determine the variation of Lorenz number for Ir film with respect to temperature. In the end, the thermal transport in DNA fibers will be evaluated in detail.

3.1. DNA-promoted electron transport in Ir film on DNA fiber

Fig. 2(a) presents the electrical resistivity against temperature for two bulk Ir (data from Selbach [25] and White [26]) and for two DNA fibers coated with Ir film in this work. The electrical resistivity of the Ir film is calculated out based on the measured electrical resistance, sample length, diameter, and the thickness of the Ir film. As we can see, the electrical resistivities of bulk Ir and Ir films are all proportional to the temperature at high temperatures (above 50 K). The rates of change of electrical resistivity with temperature are identical. Below 50 K, the electrical resistivity starts to approach a certain value. This value is entitled "residual electrical resistivity" and is caused by electron scattering by grain boundaries, static impurities and defects, which is essentially temperature independent. The residual electrical resistivities of the two Ir films are 2.20×10^{-7} Ωm and 3.22×10^{-7} Ωm, much larger than those of bulk Ir (almost zero). This is due to the increased electron scattering by the increased grain boundaries, impurities and defects when the Ir film is ultra-thin.

The electrical resistivity can be obtained by the addition of the residual electrical resistivity ρ_0 and the intrinsic electrical resistivity ρ_i that is $\rho = \rho_0 + \rho_i$. The intrinsic electrical resistivity is caused by thermal vibrations of the lattice (phonons), and thus shows temperature dependent behavior. The shape of the electrical resistivity ρ against temperature curve is characterized by the Bloch-Grüneisen formula,

$$\rho = \rho_0 + \alpha_\rho \left(\frac{T}{\theta_R}\right)^5 \int_0^{\theta_R/T} \frac{x^5}{(e^x - 1)(1 - e^{-x})} dx, \tag{5}$$

where α_ρ is a constant and θ_R is the Debye temperature. α_ρ is proportional to $\lambda_{tr}\omega_D/\omega_p^2$, where λ_{tr} is the electron-phonon coupling constant, ω_D is the Debye frequency, and ω_p is the Drude plasma frequency [27].
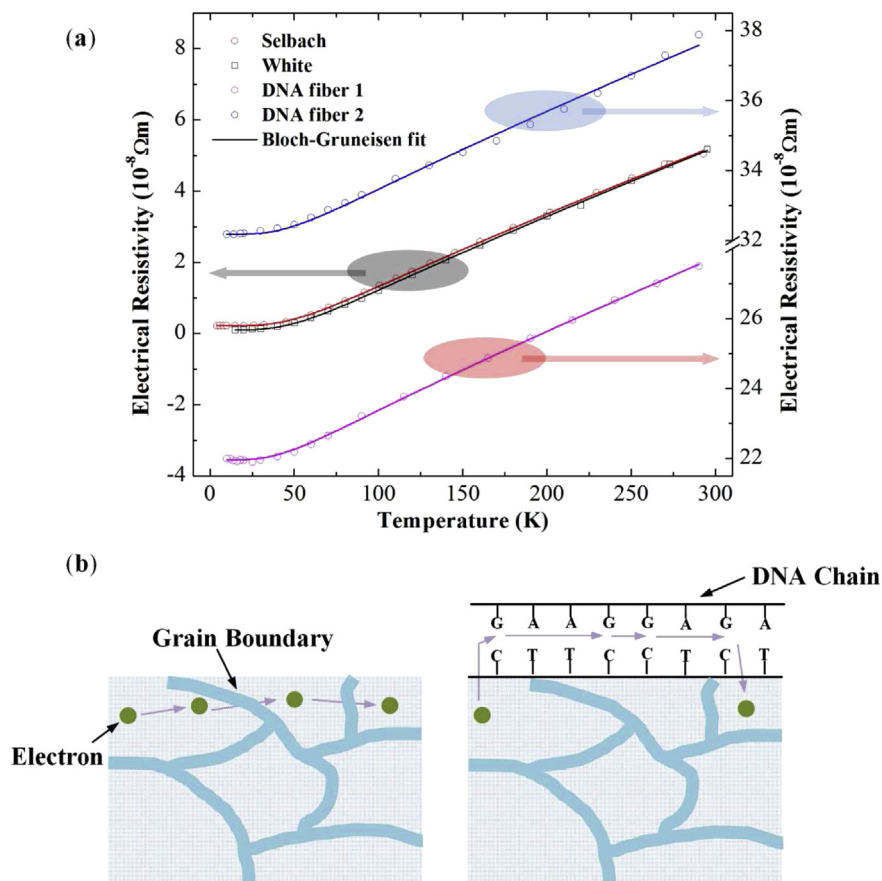
Fig. 2. (a) Electrical resistivity of bulk Ir and nanoscale Ir film versus temperature. Solid curves are Bloch-Grüneisen fits. (b) Schematic of electron scattering from grain boundaries and transfer along DNA chains.

The solid lines in Fig. 2(a) are fits to the measurements by using Eq. (5). The fitting has two parameters: α_ρ and θ_R. For two bulk Ir, the fitting results are: 21.86×10^{-8} Ωm and 22.34×10^{-8} Ωm for α_ρ, and 306.1 K and 307.6 K for θ_R. These values are consistent with each other. The Debye temperatures obtained are lower than the values extracted from the low temperature specific heat measurement (420K) [28], but close to the specific heat measurement made in the approximate range $\theta_R/2$ to θ_R, i.e. high-temperature value (290 K) [29]. The fitting results for two Ir films on the DNA fiber sample are: 21.96×10^{-8} Ωm and 22.49×10^{-8} Ωm for α_ρ, 259.4 K and 285.9 K for θ_R. The Debye temperature values show a reduction by 7–15%. This behavior is caused by phonon softening (more amorphous structure) at the grain boundaries in the Ir film. The reduction of the Debye temperature indicates a general reduction in frequency of the transversal-acoustic (TA) modes with respect to the corresponding modes of crystalline Ir. The reduction of the TA modes must be caused by decreased bond-bending forces in the amorphous structure. Nevertheless, the small reduction on Debye temperature has little effect on the intrinsic electrical resistivity. This is reflected by the fact that the rates of change of electrical resistivity with temperature are identical for bulk Ir and Ir film at high temperatures, shown in Fig. 2(a).

In the above analysis, we have found that the intrinsic electrical resistivity of the nanoscale Ir film is the same for bulk Ir. The identical electrical behavior against temperature seems expected, but it is not the case for Ir film on other materials we have tested, such as glass fiber, milk weed, and spider silk (data are not shown). At high temperatures (>50 K), the curve slope of temperature dependent electrical resistivity for Ir film on those materials is around 1.0×10^{-10} Ωm/K, smaller than that for bulk Ir

$(2.1 \times 10^{-10}$ Ωm/K). We then reexamine the fitting with the Block-Grüneisen formula for those samples, and find that the fitted parameters give similar θ_R but smaller α_ρ, with respect to the fitting results for DNA fiber samples. We propose that the electron scattering by grain boundaries in nanoscale Ir film is appreciable, which will indeed result in different electrical behaviors other than bulk Ir. However, DNA chains have the capability of transferring electrons over around ten nm by thermal hopping and quantum tunneling. This provides extra channels for electron transport other than through grain boundaries in the Ir film. The schematic of this physical process is shown in Fig. 2(b). The alternative paths of electrons preserve similar electrical behavior of Ir film on DNA fiber as bulk Ir. However, for other substrate materials, the electrons have no options but to transmit through the grain boundaries, leading to very different electron conduction behaviors. Since it is speculated that DNA chains provide extra channels for electron transport, the contact resistivity at the Ir-DNA interface is also believed small to unblock the channels between Ir and DNA. However, at this point we have no evidence on determining the contact resistivity. This could be important in our future work to fully understand the electron transport mechanism in DNA supported Ir films. In addition, the total contact resistance is also speculated negligible due to large Ir coating area on supported DNA fiber.

3.2. Lorenz number determination for the Ir film

3.2.1. Lorenz number determination at room temperature

To obtain the thermal conductivity and diffusivity of the DNA fiber, the Ir coating and radiation effects should be appropriately estimated in the expressions of effective thermal conductivity and

diffusivity. The radiation effect can be calculated easily. For precisely estimating the Ir coating effect, the Lorenz number L_{Ir} for Ir over a wide temperature range is needed. However, the Lorenz number for the nanoscale Ir film may be different from the bulk's value. Huan et al. discovers that the Lorenz number is 7.08×10^{-8} WΩ/K² for 0.6 nm thick Ir film [24] and 7.44×10^{-8} WΩ/K² for 6.4 nm gold film [30] at room temperature. Both tests are carried out on glass fiber substrates. The twofold increase from the bulk's value of the Lorenz number is explained by a much stronger reduction in electrical conductivity than thermal conductivity at grain boundaries in nanoscale films. Therefore, the Lorenz number for bulk Ir is not used in this work directly. Instead, the TET technique is capable of measuring the Lorenz number for Ir nanoscale film. We successfully measure the Lorenz number for Ir nanoscale film on DNA fiber at room temperature. However, under reduced temperatures, it is hard to keep the fiber structure unchanged during the cooling and heating processes, and the sample always ends up with no resistance reading, indicating that the Ir film does not stay on the DNA fiber continuously any more. Nevertheless, with the Lorenz number precisely measured at room temperature, we are able to derive an expression of Lorenz number as a function of temperature for Ir nanoscale film.

First of all, the DNA fiber is coated with a 15 nm-thick Ir film, and the TET measurement is conducted to measure its thermal diffusivity. Then another 5 nm-thick Ir film is coated on the top of the previous Ir film, and TET measurement is conducted again. It can be derived from the expression of $\alpha_{real+rad+Ir}$ that the change of $\alpha_{real+rad+Ir}$ is proportional to the change of $1/R$ due to the addition of the Ir film:

$$\Delta\alpha_{real+rad+Ir} = \frac{L_{Lorenz}Tl}{A\rho c_p} \cdot \Delta\left(1/R\right). \qquad (6)$$

If we consider the TET characterization for 15 nm Ir film as the base test, the following measurements from 20 nm to 40 nm can be used to subtract the base test, and the change of $\alpha_{real+rad+Ir}$ against the change of $1/R$ is plotted and shown in the inset of Fig. 3. The slope of the fitting line is determined as 2.8×10^{-5} m² Ω/s. With other known parameters, the Lorenz number for 5 nm Ir film on the DNA fiber at room temperature is determined to be 2.38×10^{-8} WΩ/K². This value is fairly close to the Lorenz number for bulk Ir, 2.58×10^{-8} WΩ/K² [31], and much lower than that of the ultrathin Ir film on glass fibers discovered by Huan et al. For ultrathin metallic films, either supported or free-standing, the inside nanocrystalline nature will significantly reduce the electron and thermal transport. Quantum mechanical reflection of electrons at the grain boundaries reduces the electrical conduction further than the thermal conduction. This leads to a Lorenz number much higher than that of the bulk counterpart. However, in the Ir film on DNA fiber, the electron transport is promoted with DNA chain. This phenomenon results in similar Lorenz number values between bulk Ir and Ir film on DNA fiber.

3.2.2. Lorenz number at reduced temperatures

To determine the expression of Lorenz number as the function of temperature, we start with the well-known Wiedeman-Franz law,

$$L = \frac{\rho}{WT}, \qquad (7)$$

where ρ is the electrical resistivity, and W is the thermal resistivity (inverse of thermal conductivity κ_{el}). The thermal resistivity is $W = \kappa_{el}^{-1} = 3m/(\pi^2 n k_B^2 T\tau)$ [28], where m is the electron mass; n is the electron density; k_B is the Boltzmann constant; T is temperature; and τ is the relaxation time. Instead of looking at W, we define a unified thermal resistivity: $\Theta = WT$, which only changes with $1/\tau$
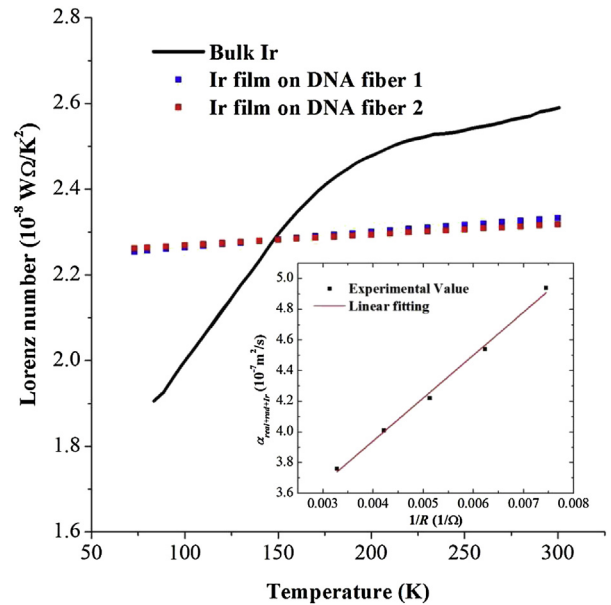
Fig. 3. Variation of the Lorenz number with temperature for bulk Ir and Ir nanoscale film on DNA fibers. Inset: Linear fitting (solid line) of the effective thermal diffusivity ($\alpha_{real+rad+Ir}$) against the electrical conductance ($1/R$) for Ir film on the DNA fiber. The slope of the fitting line is determined as 2.8×10^{-5} m² Ω/s. Then the Lorenz number for 5 nm Ir film on the DNA fiber at room temperature is determined to be 2.38×10^{-8} WΩ/K².

proportionally for the same metal. In this way, the unified thermal resistivity plays the same critical role as the electrical resistivity (also proportional to $1/\tau$) to reflect the electron scattering in metals.

Based on the electrical resistivity study, we have observed that the intrinsic electric resistivity is very close to that of bulk Ir. So it is physically reasonable to take the intrinsic unified thermal resistivity of Ir nanoscale film on DNA fiber is the same as that for bulk Ir. Therefore, the Lorenz number for Ir nano-film on DNA fiber can be related to that for bulk Ir, as

$$L_{Ir} = \frac{\rho_{bulk} + \rho_e}{\Theta_{bulk} + \Theta_e} = \frac{\rho_{bulk} + \rho_e}{\Theta_{bulk} + \rho_e/L_e}, \qquad (8)$$

where ρ_e, Θ_e are the extra residual electrical and unified thermal resistivities on top of bulk Ir, respectively, and $L_e = \rho_e/\Theta_e$. To our best knowledge, the only available electrical and thermal resistivity data extracted from the same bulk Ir sample is given in Ref. [32]. The resistivity data are over an approximate temperature range 80−300 K, not down to low temperatures. There is one advantage to deal with resistivity during this temperature range: both ρ_{bulk} and Θ_{bulk} are proportional to temperature. Thus, the resistivity data for bulk Ir in 80−300 K can be fitted as:

$$\rho_{bulk} = 0.02015T - 0.87711 \times 10^{-8}\,\Omega\text{m} \qquad 9(a)$$

$$\Theta_{bulk} = 0.00711T - 0.13977\,\text{mK}^2/\text{W} \qquad 9(b)$$

Note that the resistivity data will start to show non-linear characteristics for temperature below 80 K. Thus in general situations, Eq. (9) a and b are only valid to derive Lorenz number variation with temperature for Ir film in the temperature range of 80−300 K. For temperature below 80 K, these equations fail to capture the variation. The extra electrical residual resistivity (ρ_e) is the difference between the electrical resistivity of the Ir film and the electrical resistivity of bulk Ir at the same temperature. L_e is taken constant for our samples and is determined by the Lorenz

number measurement at room temperature. The measurement gives values of 6.83×10^{-8} Ωm for ρ_e and 3.05 mK²/W for Θ_e. Thus, L_e is 2.28×10^{-8} WΩ/K². Afterwards, we use Eq. (8) to evaluate the Lorenz number for nanoscale Ir film at reduced temperatures. For example, ρ_e for DNA fiber 1 is 22.53×10^{-8} Ωm at room temperature. Thus, the Lorenz number for this sample can be evaluated as

$$L_{Ir} = \frac{0.02015T - 0.87711 + 22.53}{0.00711T - 0.13977 + 9.8816}$$
$$= \frac{0.02015T + 21.6545}{0.00711T + 9.7425} \times 10^{-8} \text{WΩ/K}^2 \quad (10)$$

Fig. 3 shows the Lorenz number for Ir film on DNA fibers and bulk Ir. It can be seen that the Lorenz number of the Ir film decreases with decreased temperature. However, this reduction is very small, only around 2%. The Lorenz number can be seen as a constant over a wide temperature range. This result is very close to that of Ir film coated on cellulose fibers we have finished (not published yet). This is very different from the Lorenz number for bulk Ir, which has a larger reduction when temperature decreases. The difference stems from the fact that the large portion of residual resistivity in the resistivity for Ir film. Thus, the Lorenz number for Ir film is dominated by the static impurities, which has a constant Lorenz number independent of temperature. For temperatures below 80 K, the intrinsic resistivity becomes even smaller. Therefore, we can extrapolate that the Lorenz number of nanoscale Ir film is a constant at low temperatures.

3.3. Thermal transport in DNA fiber

Two DNA fibers are measured in the same manner down to 10 K. DNA fiber 1 is discussed here to show the data reduction process. The test temperatures are divided into three regions. For temperatures above 50 K, a linear correlation between temperature and resistance is adopted. With the sample size, TCR can be interpreted as 1.733 Ω/K from Fig. 2(a). The standard error of TCR is ±0.019 Ω/K. With this TCR, the temperature rise due to heating in the TET test can be obtained based on the observed resistance increase by joule heating. For example, at 190 K, the average resistance increase is 17.4 Ω. Thus, the temperature rise is found to be 10 K. As a result, $k_{real+rad+Ir}$ is calculated as 0.44 W/m·K by Eq. (2). To solve for $\alpha_{real+rad+Ir}$, the raw voltage data is normalized and fitted with the theoretical solution, shown in Fig. 4 (presented in log axis). The uncertainty of the fitting process is illustrated by plotting another two theoretical curves with ±15% variation of $\alpha_{real+rad+Ir}$. It is conclusive that the percentage uncertainty of the fitting process is within ±15%. The TET measurements are done multiple times under the same circumstance to obtain an average value of $\alpha_{real+rad+Ir}$. The average $\alpha_{real+rad+Ir}$ at 190 K for this sample is 6.05×10^{-7} m²/s. The percentage uncertainty (repeatability) is ±6% for the average $\alpha_{real+rad+Ir}$. With $k_{real+rad+Ir}$ and $\alpha_{real+rad+Ir}$, ρc_p at 190 K is calculated to be 7.3×10^5 J/m³K by Eq. (6). Consequently the percentage uncertainty of ρc_p is ±6.11%. All results under temperatures above 50 K can be processed in the same way.

For temperatures between 20 K and 50 K, we do not solve for $k_{real+rad+Ir}$ first due to a large uncertainty in determining TCR. Instead, ρc_p at low temperatures are linearly extrapolated from the values obtained for the high temperature region [Fig. 5(c)]. $\alpha_{real+rad+Ir}$ is solved in the same manner as that for temperatures above 50 K. Then $k_{real+rad+Ir}$ is obtained by multiplying $\alpha_{real+rad+Ir}$ with ρc_p. For temperatures below 20 K, The sample needs to be heated till around 50 K to obtain a distinct TET signal. For such wide temperature range, the TCR cannot be considered constant. As a result, the TET technique is not applicable due to the very strong non-linear $I-V$ effect. Therefore, we do not report the thermal
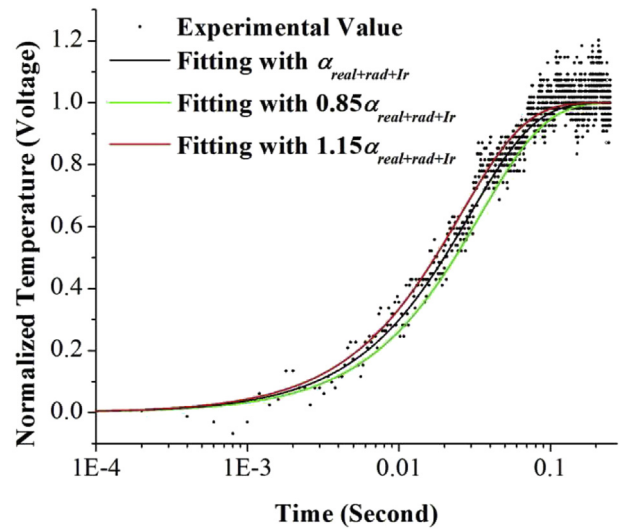

Fig. 4. TET fitting (solid black line) for DNA fiber 1 at 190 K. The uncertainty of the fitting is demonstrated by comparing two fitting curves with ±15% variation of the effective thermal diffusivity ($\alpha_{real+rad+Ir}$).

properties of DNA fiber below 20 K, although the electrical resistivity of Ir film is reported in that temperature range. The thermal properties of DNA fiber 2 are reported down to 20 K for the same reason.

After excluding the Ir and radiation effects, we are able to determine the variations of thermal conductivity, thermal diffusivity, and volumetric heat capacity of DNA fibers with
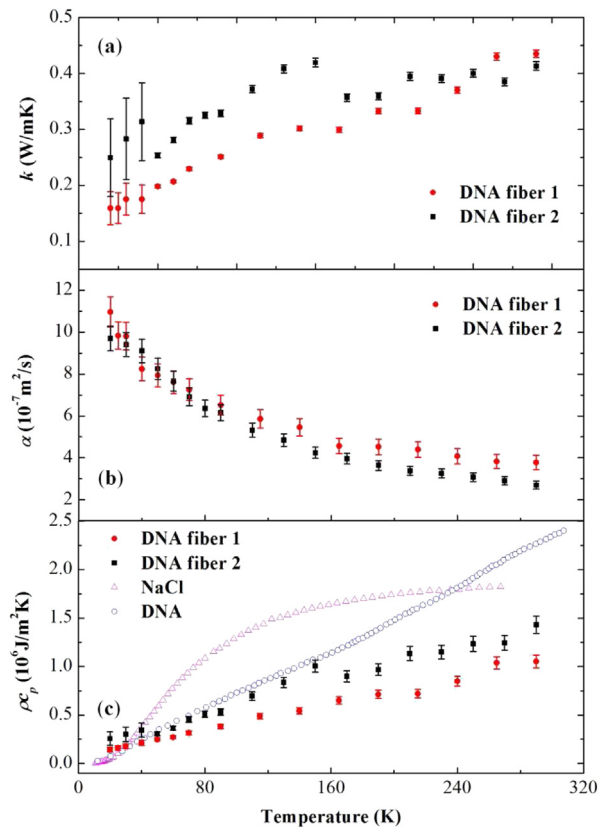

Fig. 5. Variations of thermal conductivity, thermal diffusivity, and volumetric heat capacity of DNA fibers with temperature. The uncertainties are presented as error bars.

temperature, as shown in Fig. 5(a)–(c), respectively. The uncertainties of the measurements are presented as error bars. Two DNA fibers have similar results. At room temperature, the thermal conductivity of the DNA fibers is 0.42 W/m·K, close to the result we obtained before (0.33 W/m·K). As temperature goes down, the thermal conductivity gradually decreases. In contrast, the thermal diffusivity increases as temperature decreases. At room temperature, the thermal diffusivity is 3–4×10^{-7} m/s^2. As temperature approaches 20 K, the thermal diffusivity increases to around 1–1.1×10^{-6} m/s^2. The volumetric heat capacity of the DNA fibers is proportional to temperature, and approaches zero at low temperature. Generally, the thermal conductivity of DNA fiber 1 is lower, and the thermal diffusivity of both fibers is similar. This leads to a lower volumetric heat capacity of DNA fiber 1. This can be explained by the reduction of density for DNA fiber 1 due to more air voids inside.

With the variations of thermal properties with temperature for DNA fiber, we are able to answer the following question: is the DNA fiber crystalline NaCl-DNA composite or pure DNA bundle? The answer is pure DNA bundle. First of all, it is clear that NaCl crystallites are not observed in the SEM images [Fig. 1(a)]. To make a more persuasive conclusion, we compare the characterization of thermal properties of DNA fiber and NaCl [33] against temperature. The thermal conductivity of NaCl increases with the decreasing temperature for high temperatures, and reaches the maximum value around 1000 W/m K at about 10 K. Then the thermal conductivity drops with the decreasing temperature. This variation is different from that of DNA fiber, and the magnitude of thermal conductivity for NaCl is way higher. The variations of thermal diffusivity are similar, but the magnitude for NaCl is 10–100 times larger. In the end, we turn our attention to the comparison of volumetric heat capacities, whose magnitudes are in the same order. In Fig. 5(c), temperature dependence of the volumetric heat capacities of NaCl, DNA fibers and native strands of Na-DNA [34] of salmon sperm are presented. The density of native strands of Na-DNA is chosen as 1.407×10^3 kg/m^3 [35]. The heat capacity curve of NaCl is typical. At high temperatures, the heat capacity approaches a constant. At very low temperatures, the heat capacity obeys the famous Debye T^3 law. In contrast, the heat capacity of DNA fibers in this work and native strands of Na-DNA are proportional to temperature over temperatures up to 300 K. The reduction of heat capacity of DNA fibers than native DNA strands is also due to the reduction of density, as explained above. With all evidence, we can make a strong conclusion that the DNA fiber sample studied in this work is indeed DNA bundle, with negligible NaCl crystals.

3.4. New defined parameter: thermal reffusivity

Under single relaxation time approximation, the phonon thermal conductivity κ_{ph} can be expressed as $\kappa = Cv^2\tau/3$. Here C is the volumetric heat capacity ($=\rho c_p$) and v is the average phonon speed which changes little with temperature. τ is the relaxation time. As the thermal diffusivity is defined as $\alpha = k/\rho c_p$, we could have $\alpha^{-1} = 3v^{-2}\tau^{-1}$. According to Matthiessen's rule, $\tau^{-1} = \tau_0^{-1} + \tau_U^{-1}$, where the subscripts "0" and "U" are for defect-induced scattering and phonon–phonon scattering (Umklapp processes). Thus, the inverse of thermal diffusivity can be written as the addition of residual part and intrinsic part, that is $\alpha^{-1} = \alpha_0^{-1} + \alpha_U^{-1}$. We introduce the inverse of phonon thermal diffusivity as a new parameter: thermal reffusivity. This parameter can be used to identify the thermal resistivity in DNA fiber that is caused by fiber structure imperfections and by phonon–phonon scatterings. Fig. 6 shows the variation of thermal reffusivity with temperature for the two DNA fibers. It can be seen that α^{-1} increases almost linearly with increasing temperature. This is due to the fact that $\tau_U^{-1} \propto T$ since the
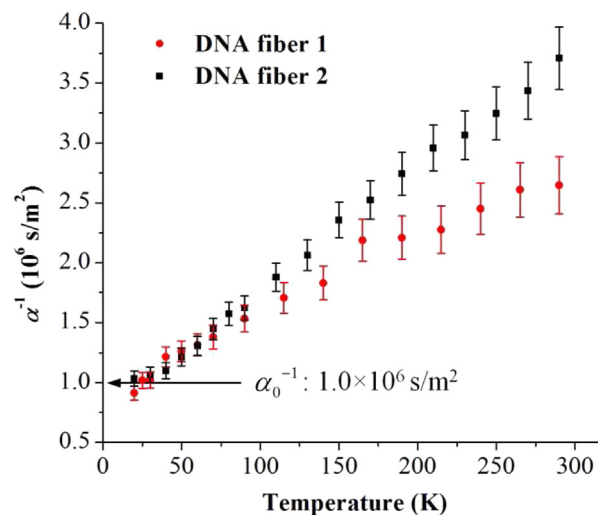

Fig. 6. Variation of thermal reffusivity with temperature for DNA fibers. The residual thermal reffusivity is determined to be 1.0×10^6 s/m^2 for both fibers.

phonon density increases almost linearly with temperature when the temperature is not very low. We also examine the thermal reffusivity theory in some bulk materials, where phonon dominates the thermal transport process, such as silicon, germanium, NaCl and NaF. It is found that they all show very similar behavior as the DNA fiber. The only difference is that α_0^{-1} is close to zero for these materials because the defects in these bulk materials are very rare. At room temperature, α^{-1} is about 2.6×10^6 and 3.7×10^6 s/m^2 for the two DNA fibers, respectively. The residual part: α_0^{-1} for both fibers is around 1.0×10^6 s/m^2. This indicates that at room temperature the intrinsic thermal reffusivities are 1.6×10^6 and 2.7×10^6 s/m^2, respectively. Then the corresponding intrinsic thermal diffusivities of defect-free fiber can reach 6.3 and 3.7×10^{-7} m/s^2. So the intrinsic thermal diffusivity is 61% and 36% higher than the measured effective values. This is the prediction of the ultimate potential for the thermal transport in DNA fibers.

With the residual thermal reffusivity, we are able to determine the structure domain size for phonon diffusion/scattering: l_s. This parameter shows the mean free length that phonon can be scattered by structural domains. The average sound velocity is estimated as $v = (1/3v_L^3 + 2/3v_T^3)^{-1/3}$, where v_L and v_T are the longitudinal and transverse sound velocities (3800 m/s and 3700 m/s in oriented DNA fiber, respectively [36]). As a result, l_s is 0.8 nm for DNA fiber. This value is reasonable since it is comparable to one base pair (0.34 nm) length and DNA double helix width (2 nm).

4. Conclusion

In this work, the energy and electron transport in nanometer-thick Ir film supported by a DNA fiber and the phonon transport sustained by the DNA itself were extensively studied under low temperatures. Compared to bulk Ir, the Ir film on DNA fiber has similar intrinsic electrical resistivity and much larger residual electrical resistivity. By fitting with the Block-Grüneisen formula, we found that the Debye temperature of Ir film shows a very small (7–15%) reduction from bulk Ir. This behavior can be explained by phonon softening. The similar intrinsic electrical resistivity of Ir film is preserved by the thermal hopping and quantum tunneling characterization of DNA chains. The electron scattering by grain boundaries in Ir film will result in different electrical behaviors other than bulk Ir, but DNA chains provide extra channels for

electrons other than grain boundaries. Afterwards, we determined the Lorenz number of Ir film as a function of temperature. At room temperature, the Lorenz number (2.38×10^{-8} WΩ/K^2) is close to that of bulk crystalline Ir (2.58×10^{-8} WΩ/K^2). Despite the fact that the nanocrystalline structure in the ultrathin metallic film will lead to a higher Lorenz number than that of bulk counterpart since it reduces the electrical conductivity further than the thermal conductivity, the electron transport promotion in Ir film on DNA fiber preserves a similar Lorenz number. With the above electrical resistivity study, we found that the Lorenz number of the Ir film is dominated by the static impurities. This leads to a constant Lorenz number over a wide temperature range. This behavior is very different from the Lorenz number for bulk Ir, where the electron-phonon scatterings play a more important role. By measuring the variations of thermal conductivity, thermal diffusivity and volumetric heat capacity with temperature, we made a strong conclusion that the DNA fiber sample studied is indeed a DNA bundle with negligible NaCl crystals inside. A new parameter, entitled "thermal reffusivity", was defined to identify the phonon thermal resistivities caused by static imperfections and phonon−phonon scatterings. From the variation of thermal reffusivity with temperature for the two DNA fibers, we found that the thermal diffusivity of defect-free DNA fiber can be promoted by around 36−61%. This new defined parameter can be widely used to predict the phonon thermal transport potential of defect-free materials. With the residual thermal reffusivity, the structure domain size determined by phonon scattering/diffusion is 0.8 nm in DNA.

Acknowledgment

References

[1] Mirkin CA, Letsinger RL, Mucic RC, Storhoff JJ. Nature 1996;382(6592):607−9.
[2] Alivisatos AP, Johnsson KP, Peng XG, Wilson TE, Loweth CJ, Bruchez MP, et al. Nature 1996;382(6592):609−11.
[3] Braun E, Eichen Y, Sivan U, Ben-Yoseph G. Nature 1998;391(6669):775−8.
[4] Berlin YA, Burin AL, Ratner MA. J Am Chem Soc 2001;123(2):260−8.
[5] Giese B, Amaudrut J, Kohler AK, Spormann M, Wessely S. Nature 2001;412(6844):318−20.
[6] Yu ZG, Song XY. Phys Rev Lett 2001;86(26):6018−21.
[7] Renger T, Marcus RA. J Phys Chem A 2003;107(41):8404−19.
[8] Zhang X, Wei SY, Haldolaarachchige N, Colorado HA, Luo ZP, Young DP, et al. J Phys Chem C 2012;116(29):15731−40.
[9] Gu HB, Guo J, Zhang X, He QL, Huang YD, Colorado HA, et al. J Phys Chem C 2013;117(12):6426−36.
[10] Zhang X, Zhu JH, Haldolaarachchige N, Ryu J, Young DP, Wei SY, et al. Polymer 2012;53(10):2109−20.
[11] Zhu JH, Chen MJ, Qu HL, Zhang X, Wei HG, Luo ZP, et al. Polymer 2012;53(25):5953−64.
[12] Gu HB, Guo J, Yan XR, Wei HG, Zhang X, Liu JR, et al. Polymer 2014;55(17):4405−19.
[13] de Pablo PJ, Moreno-Herrero F, Colchero J, Gomez-Herrero J, Herrero P, Baro AM, et al. Phys Rev Lett 2000;85(23):4992−5.
[14] Fink HW, Schonenberger C. Nature 1999;398(6726):407−10.
[15] Kasumov AY, Kociak M, Gueron S, Reulet B, Volkov VT, Klinov DV, et al. Science 2001;291(5502):280−2.
[16] Porath D, Bezryadin A, de Vries S, Dekker C. Nature 2000;403(6770):635−8.
[17] Cai LT, Tabata H, Kawai T. Appl Phys Lett 2000;77(19):3105−6.
[18] Velizhanin KA, Chien CC, Dubi Y, Zwolak M. Phys Rev E 2011;83(5):050906.
[19] Savin AV, Mazo MA, Kikot IP, Manevitch LI, Onufriev AV. Phys Rev B 2011;83(24):245406.
[20] Kodama T, Jain A, Goodson KE. Nano Lett 2009;9(5):2005−9.
[21] Xu Z, Xu S, Tang X, and Wang X. 2014;4(1):017131.
[22] Guo JQ, Wang XW, Wang T. J Appl Phys 2007;101(6):063537.
[23] Feng XH, Huang XP, Wang XW. Nanotechnology 2012;23(18):185701.
[24] Lin H, Xu S, Wang X, and Mei N. 2013;9(15):2585−2594.
[25] Selbach E, Jacques H, Eiermann K, Lengeler B, Schilling W. Thin Solid Films 1987;149(1):17−28.
[26] White GK, Woods SB. Philos Tr R Soc S-A 1959;251(995):273−302.
[27] Chelikowsky JR, Louie SG. Quantum theory of real materials. Boston: Kluwer Academic Publishers; 1996.
[28] Kittel C. Introduction to solid state physics. 8th ed. Hoboken, NJ: J. Wiley; 2005.
[29] Clusius K, Losa CG. Z Naturforsch Pt A 1955;10(7):545−51.
[30] Lin H, Xu S, Li C, Dong H, and Wang X. 2013;5(11):4652−4656.
[31] Powell RW, Tye RP, Woodman MJ. J Less-Common Met 1967;12(1):1−10.
[32] Powell RW, Tye RP, and Woodman MJ. 1962;6(4):138−143.
[33] Purdue University Thermophysical Properties Research Center, Touloukian YS. Thermophysical properties of matter. The TPRC data series. New York: IFI/Plenum; 1970.
[34] Mrevlishvili GM. Thermochim Acta 1998;308(1−2):49−54.
[35] Smialek MA, Jones NC, Hoffmann SV, Mason NJ. Phys Rev E 2013;87(6).060701(R).
[36] Maret G, Oldenbourg R, Winterling G, Dransfeld K, Rupprecht A. Colloid Polym Sci 1979;257(10):1017−20.